PNNL-15576

Pacific Northwest
National Laboratory
Operated by Battelle for the
U.S. Department of Energy

Long Wave Infrared Cavity Enhanced Sensors

M. S. Taubman
D. C. Scott
B. D. Cannon
T. L. Myers
J. T. Munley
V. T. Nguyen
J. F. Schultz

December 2005

Prepared for the U.S. Department of Energy
under Contract DE-AC05-76RL01830

DISCLAIMER

PACIFIC NORTHWEST NATIONAL LABORATORY
operated by
BATTELLE
for the
UNITED STATES DEPARTMENT OF ENERGY
under Contract DE-AC05-76RL01830

Printed in the United States of America

Available to DOE and DOE contractors from the
Office of Scientific and Technical Information,
P.O. Box 62, Oak Ridge, TN 37831-0062;
ph: (865) 576-8401
fax: (865) 576-5728
email: reports@adonis.osti.gov

Available to the public from the National Technical Information Service,
U.S. Department of Commerce, 5285 Port Royal Rd., Springfield, VA 22161
ph: (800) 553-6847
fax: (703) 605-6900
email: orders@ntis.fedworld.gov
online ordering: http://www.ntis.gov/ordering.htm

This document was printed on recycled paper.
(9/2003)

PNNL-15576

Long Wave Infrared Cavity Enhanced Sensors

M. S. Taubman
D. C. Scott
B. D. Cannon
T. L. Myers
J. T. Munley
V. T. Nguyen
J. F. Schultz

December 2005

Prepared for
the U.S. Department of Energy
under Contract DE-AC05-76RL01830

Pacific Northwest National Laboratory
Richland, Washington 99352

Summary

The principal goal of Pacific Northwest National Laboratory's (PNNL's) long wave infrared (LWIR) cavity enhanced sensor (CES) task is to explore ultra-sensitive spectroscopic chemical sensing techniques and apply them to detecting proliferation of weapons of mass destruction (WMD). Our primary application is detecting signatures of WMD production, but LWIR CES techniques are also capable of detecting chemical weapons. The LWIR CES task is concerned exclusively with developing novel point sensors; stand-off detection is addressed by other PNNL tasks and projects. PNNL's LWIR CES research is distinguished from that done by others by the use quantum cascade lasers (QCLs) as the light source. QCLs are novel devices, and a significant fraction of our research has been devoted to developing the procedures and hardware required to implement them most effectively for chemical sensing. This report details the progress we have made on LWIR CES sensor development.

During earlier years (FY02-03), PNNL investigated QCL-based cavity-enhanced sensing architecture ranging from simple direct absorption through an advanced form of laser-based spectrometry known as noise-immune cavity-enhanced optical heterodyne molecular spectroscopy (NICE-OHMS), the latter giving us an exceptional sensitivity of around 1×10^{-10} cm^{-1} $(Hz)^{-1/2}$. Different modes of sensor operation were explored in order to optimize both sensitivity and selectivity for a first round of fieldable sensor development in the LWIR. This included such things as the choice of architecture itself, and whether to use Lamb dips rather than Doppler profiles as target features. Ultimately, the intermediate architecture of FM recovery cavity-dither detection was chosen over NICE-OHMS due to the difficulty of reproducibly phase modulating QCLs at hundreds of megahertz (MHz). The use of the larger more common Doppler features was also chosen over Lamb dips because of increased operating pressures, tens of Torr rather than tens of milliTorr, making a large difference in operational complexity and speed of the resulting sensor. The latter choice also removed the possibility of reducing sensitivity through gross over saturation, which can happen in the LWIR at low analyte pressures for even moderate optical powers. FY04 saw considerable planning for the transition to fieldable sensor development, including the selection of appropriate target gases and spectra, designing a ring cavity to replace the linear cavity allowing reduced component count and sensor footprint, designing new piezo mirror mounts to facilitate the deeper cavity dither necessary for the recovery of Doppler features rather than Lamb dips, modification of mechanical systems including major redesign of our QCL laser dewars, and finally, refinement of required electronics, in particular the QCL current controllers.

During FY05, the modifications envisioned in FY04 were implemented and successfully tested. The ring cavity architecture shows promising immunity to optical fringing, one of the most insidious limitations for any chemical sensor operating in the LWIR. The deep dither piezo mirror mounts were constructed and successfully tested. The results from tests of the modified dewars show outstanding pointing stability compared to earlier performance. Development of a superior current controller for QCL operation, which has continued over several years, has been completed with outstanding results. During the year, there were problems in development of the optical ring cavity, requiring unforeseen dedication of time and resources. This combined with a reduced level of funding, resulted in the delay of planned milestones for FY05, including the developing the automatic locking system necessary for autonomous field operation of a cavity-locked sensor, and the first deployment an LWIR QCL sensor late in the year. With increased funding these milestones could be met in FY06.

Contents

Figures

1.0 Introduction

Quantum cascade laser-based cavity-enhanced sensors have been under development in the long wave infrared (LWIR) at PNNL now since FY02. Various bench top cavity-enhanced sensor (CES) architectures were researched, designed, built and examined. Over this time, the tremendous potential of this technology has become apparent, with the capability to measure down to parts per trillion (ppt) relative concentrations, quickly and accurately. The goal of finding better and more sensitive ways of detecting weapons of mass destruction remains of paramount importance. LWIR CES remain one of the most appropriate technologies for this task.

1.1 The potential of LWIR CES and the advantages over GCMS

It is projected that with adequate funding, in several years LWIR CES using quantum cascade lasers (QCLs) could be deployed in small, lightweight packages, providing accurate detection of low concentration trace gases that are indicative of WMD proliferation. These sensors will also allow monitoring of facilities of interest to determine quantities and types of emissions. For each application, the optimum architecture can be chosen to provide the most suitable compromise between footprint and sensitivity, ranging from parts-per-billion (ppb) UAV mounted systems for reconnaissance purposes through to larger ultra-sensitive systems used to analyze remotely collected samples to the ppt level. Conversely, the selection of the appropriate wavelength of quantum cascade laser (QCL) from the impressive range of 3 to 25 microns, allows extremely flexible sensor design and the targeting of many molecular species with strong signatures in this region.

Continued development of sensors using this technology represents a significant improvement over existing techniques, such as Gas-Chromatograph Mass Spectrometry (GCMS). While offering superb sensitivity, GCMS has specific limitations because it does not distinguish based on the chemical behavior of a molecule, but rather the mass of its constituent atoms. Moreover, GCMS does not discriminate between isomers, or different molecules of the same mass. On the other hand the spectroscopic features of a gaseous species are highly specific and hence more reliable indicators of the presence of particular chemicals. Much greater selectivity is thus available using infrared spectroscopy. There are also many practical issues that make GCMS systems considerably more difficult to field than current cryogenic LWIR laser systems. The GCMS has long response times (>70s) while the LWIR laser systems can provide near instantaneous measurements (<1s). Detectors used in GCMS systems often include radioactive sources, which complicates shipping and deployment of the instrument especially to sensitive international sites. The radioactive sources also tend to drift with changes in temperature and pressure, which requires constant calibration with zero air using complicated computer controlled gas handling systems, heavy gas cylinders, and heavy power hungry pumps and solenoids. This calibration sequence leads to gaps in data-streams that could lead to delays or missed detection opportunities. The pumps and solenoids often generate mechanical and electrical noise that interferes with other instruments. GCMS systems are not useful for reactive species such as HCl, HF, HI, HBr, NH_3, N_2H_4, etc. The columns require constant maintenance and must be baked out to remove contaminants resulting in decreased duty cycle. In fact the clever terrorist could release a reactive gas to “poison” the GCMS columns and render

the instrument inoperative. The LWIR laser system in contrast can provide rapid response time, high duty cycle, and very high sensitivity with near zero false positive readings. A fieldable version of even a cryogenically operated LWIR CES could weigh less than 20 kg, low power consumption (<50 W) system whereas GCMS systems are heavy (>60 kg) and require high power (>300 W). When room temperature CW QCL operation becomes commonplace, this footprint will decrease considerably.

1.2 Report Layout

This report proceeds with background section 2.0 giving a brief review of the different cavity-locked architectures examined in previous years of the project, and an explanation of the choice of the FM recovery cavity-locked detection using Doppler features. The implementation of the ring cavity will be discussed in section 3.0, highlighting the advantages and particular challenges. Section 4.0 continues with the cavity dither technique, the implementation of a new mirror mount allowing the transition from Lamb dip detection to Doppler feature recovery. The results of the laser dewar modifications carried out in FY04 are given in section 5.0, while those of the ultimate version of the QCL current supply are given in section 6.0. We then wrap up with the outlook for FY06 in section 7.0 and a summary in section 8.0.

2.0 Background

2.1 Review of cavity enhanced sensor architectures

The various LWIR CES architectures built and tested at over the past several years are discussed in great detail in the FY02 report, and elaborated upon in later reports. Nonetheless, a brief summary of the various cavity-locked architectures along with their respective advantages and disadvantages are given here. Figure 2.1 depicts the full range of continuous wave (cw) cavity-locked chemical sensors studied to date at PNNL.

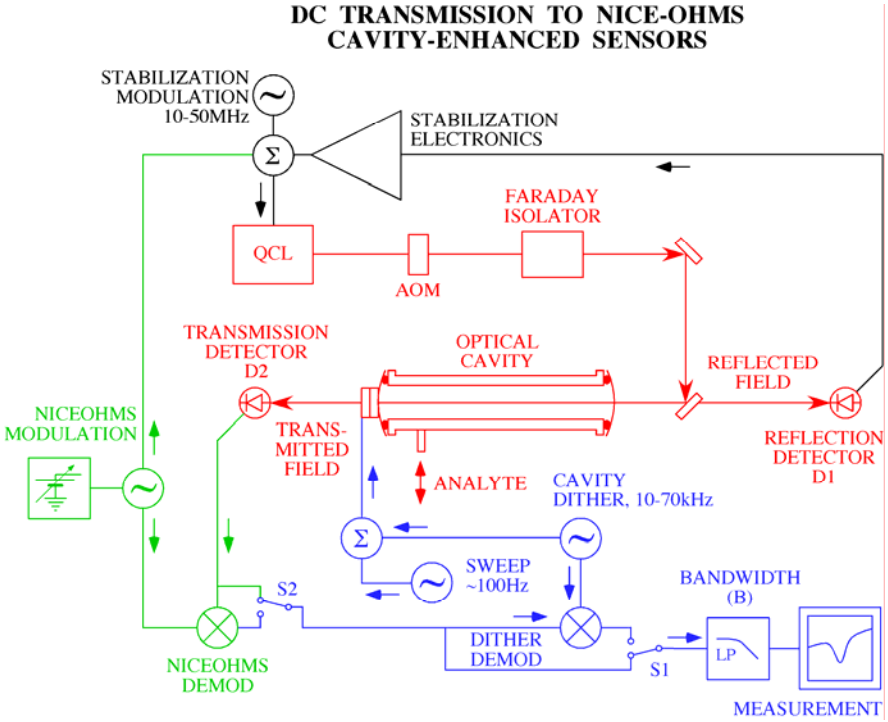

Figure 2.1. This schematic represents the range of cavity-locked sensing architectures under development at PNNL. Cavity locking is effectuated using the Pound-Drever-Hall (PDH) technique, via a modulation in the tens of megahertz, the reflection detector D1, and related stabilization electronics. The optical cavity is swept in the hundreds of hertz, forcing the laser to follow these scans over spectroscopic features of the analyte. Intra-cavity absorption causes dramatic changes in the cavity transmission, observed directly on D2 when switches S1 and S2 are as shown. By changing S1 and dithering the cavity in the tens of kilohertz, a 1-f modulation scheme is formed. By then also changing S2 and applying a high frequency modulation equal to the cavity free spectral range, the NICE-OHMS technique is realized.

In all our QCL-based LWIR CES architectures involving linear optical cavities, the optical field from the QCL is coupled into an optical cavity via an acousto-optic modulator (AOM) and a Faraday isolator in order to minimize the optical feedback into the QCL from back reflections. Reflected and transmitted light from the cavity are observed using detectors D1 and D2 respectively. In all cases the QCL is locked to a fundamental mode of an optical cavity, using the Pound-Drever-Hall (PDH) stabilization (Barger, Sorem and Hall 1973; Drever, et al. 1983; Salomon, Hils and Hall 1988). In brief, the QCL is phase-modulated in the tens of MHz, and the resulting signal appearing at the reflection detector D1 is used to vary the QCL injection current via stabilization electronics in order to keep the QCL frequency coincident with that of the cavity mode to within a very small fraction of the cavity line width. Locking a laser to an optical cavity leads naturally to line width narrowing and frequency stabilization of the laser source, which is often the reason why it is performed. Moderate amounts of line width narrowing are beneficial to chemical sensors, although when locking a QCL to even a moderate quality optical cavity in order to build such a sensor, the resulting level of line width narrowing is far in excess of that beneficial to such sensors. Although beyond the scope of this report, this side benefit is extremely useful for a wide range of other applications including the development of optical clocks, and is discussed in great detail in our publications (Taubman et al. 2002b; Williams et al. 1999; Taubman et al. 2004b).

2.1.1 DC cavity-locked sensor

The most basic QCL cavity-locked sensor architecture, depicted in Figure 2.1 with switches S1 and S2 in the positions indicated, is realized any time an analyte is introduced into an optical cavity to which a QCL is locked. The cavity length is varied over a small range via a piezo element in contact with one of the mirrors, causing the cavity mode frequency and that of the QCL to be scanned. When this scan encompasses spectral features of the analyte, absorption signals appear at the cavity transmission detector, which are filtered at some bandwidth B, measured on a digital oscilloscope. The high sensitivity of the optical cavity means that relatively small amounts on intra-cavity loss, cause large changes in the transmission signal. For very small levels of absorption, this can be thought of as an effective interaction path length enhancement of $2F/\pi$, where F is the finesse of the optical cavity. The advantages of this sensor, referred to here as the "DC cavity-locked sensor," are that it is relatively simple and it gives a direct result with a simple mathematical model that remains valid even for levels of absorption that would extinguish cavity transmission altogether. The principal disadvantage in theory of this sensor is that its sensitivity is directly limited by the low frequency amplitude noise of the laser and detector, specifically, 1/f noise.

2.1.2 FM recovery cavity-locked sensor

The next sensor architecture to be discussed is achieved by implementing frequency modulation (FM) through "dithering" the optical cavity, and adding phase-sensitive detection, depicted in Figure 2.1 by changing the position of switch S1 opposite to what is shown. We refer to this architecture as the "FM Recovery Cavity-Locked Sensor," or the "Cavity-Dithered Sensor." The cavity dither signal is applied to a piezo element attached to one cavity mirror in a similar a way to the sweep signal. In actuality, these piezo units are separate and operate on different mirrors, although they are represented here as the same unit for simplicity. The dither frequency is typically in the tens of kilohertz, and is thus well within the bandwidth of the laser locking loop (several MHz), and so the laser frequency faithfully follows this

cavity dither in the same way as it follows a cavity sweep. Depending on the harmonic of the modulation frequency used to demodulate the signal seen at detector D2, the 1-f, 2-f or in general, n-f absorption features are obtained. Advantages of FM techniques such as this include freedom from the low frequency technical noise limiting the DC cavity-locked sensor, and a strong bias in sensitivity to spectral features of a specific width, that of the FM depth. Disadvantages include a moderate increase in complexity, but the benefits far outweigh the liability. This is our principal choice of cavity-enhanced QCL-based sensor.

2.1.3 NICE-OHMS

An ultimate form of "Cavity-Enhanced sensor is that of Noise-Immune Cavity-Enhanced Molecular Spectroscopy" or NICE-OHMS, invented by Ma, Ye and Hall (Gianfrani, Fox and Hollberg 1999; Ye, Ma and Hall 1998; Ishibashi and Sasada 1999). This is based on the idea of resonant sideband detection, in which FM sidebands coincident with adjacent cavity modes are placed on the light. Noise between the laser and the optical cavity produces common-mode phase and amplitude changes in the sidebands and carrier, and hence produces no detectable signal. Molecular absorptions however, affect each the sidebands and carrier differently, producing differential phase changes and hence a detectable signal. The cavity-dither technique is usually added as a second level of modulation providing extra selectivity. This configuration is represented in Figure 2.1 with both switches S1 and S2 in the opposite positions to those shown. This technique has enormous potential, and has indeed enabled our most sensitive measurement to date of around $1x10^{-10}$ $cm^{-1}(Hz)^{-1/2}$. However, due to increased complexity and the observed differences in phase modulation behavior between different QCLs, the resulting need to change optical cavity lengths in order to accommodate this, and the loss of detector responsivity at the required high modulation frequencies, this technique has been set-aside for the moment.

2.2 The choice of FM cavity-dither Doppler-limited sensor

The FM recovery cavity-locked sensor discussed in 1.2.2 above was chosen as the principal cavity-enhanced architecture to be taken to the field due to its formidable potential sensitivity and only moderate complexity. No further discussion of the NICE-OHMS technique is presented in this report, much in depth discussion being given in the FY02 annual report (Taubman et al. 2002a). In addition to the choice of architecture, the mode of operation was also given consideration. Much of our earlier work involved the detection of Lamb dips, very narrow features whose appearance in spectra would allow fine discrimination between many species. However, to appear, Lamb dips require very low operating pressures in the tens of milliTorr (mTorr) or below, thus avoiding pressure broadening and allowing optical saturation to occur. Operating at such low pressure however, make a large difference in operational complexity and speed of the resulting sensor. It was also soon observed that over-saturation occurring at these low pressures also meant that sensitivity could be severely reduced for strongly interacting analytes. At the very least, the precision of the instrument could be compromised unless these effects were thoroughly understood for all analytes and at all operating QCL powers (Taubman et al. 2003). For these reasons, the larger more commonly used Doppler features were targeted, allowing operating pressures in the tens of Torr, much alleviating the operational concerns and removing the saturation effects via the depopulating effects of collisional broadening.

2.3 Challenges and Solutions

Several challenges remained to fielding a sensor based on this technology. These included reducing the footprint of the laboratory bench top experiments to a level appropriate for a fieldable configuration, stabilizing the laser mounting arrangement, adapting the cavity-dither technique to operate at the larger modulation depths required to recover Doppler features, to finalize power supply designs, automate the locking systems and finally, to reduce the level of optical fringing observed, which is in fact the limiting phenomenon in all our cavity-enhanced sensor architectures. To help visualize these areas of focus Figure 2.2 shows the FM recovery cavity-enhanced sensor with most of these areas highlighted in green. Most of the large optics were associated with isolating the QCL from back-reflection from the optical cavity and thus preventing disruption to the cavity lock, frequency pulling and instability. These include the AOM, the Faraday isolator, the quarter-wave rhomb (λ/4), and the wire grid polarizer. In addition to being large and heavy, these optics are also expensive, lossy, cause fringing and are difficult to obtain. Focus areas not shown in Figure 2.2 include the laser dewar and QLC power supply. Most of the challenges listed here were effectively dealt with in FY04 through FY05 and will be discussed in detail in this report.

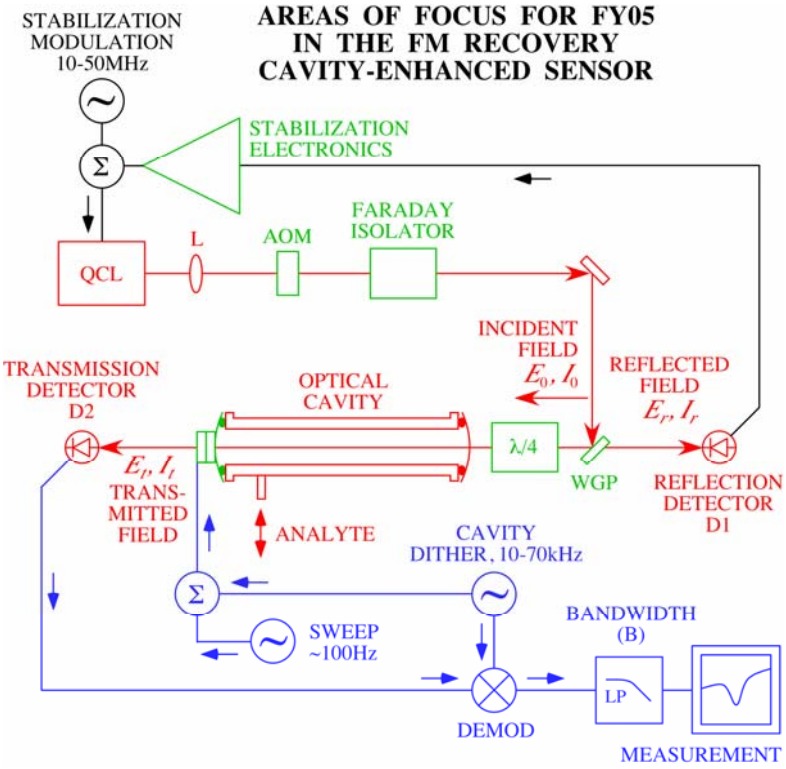

Figure 2.2. This figure depicts the FM Recovery Cavity-Locked Sensor with areas of focus in 2005 shown in green. These included trying to reduced the size of, or remove, the large optics: acousto-optic modulator (AOM), the Faraday isolator, the quarter-wave rhomb (λ/4) and the wire grid polarizer (WGP), modifying the piezo mount to achieve greater dither modulation, the stabilization electronics. Focus areas not shown include the laser dewar and QLC power supply.

Optical fringing deserves particular mention as an ongoing challenge because it produces periodic signals resembling absorption features due to interference between any two roughly parallel surfaces in communication in such a sensor. This is now especially important given our choice to pursue Doppler features, as the false signatures from fringing are typically of the spectral width of Doppler features. This phenomenon is recognized as the most insidious problem in infrared spectrometers of nearly every kind, and is a difficult problem to solve indeed. There are several ways of combating its effects some of which include rapidly dithering optics or even vibrating the optical platform on which a sensor is mounted (Hjelme, Neegård and Vartdal 1995; Webster 1985; Loewenstein et al. 2002). These techniques are somewhat difficult to implement in a cavity-locked system however because of disturbance to the cavity lock, and other techniques have to be used such as very high quality antireflection coatings, and careful optical engineering.

Due to our decision to use Doppler features rather than Lamb dips, another cavity configuration became available to use, that of a ring cavity. (Lamb dips require the collinear counter-propagating beams of a linear cavity.) This choice became a tool to fight several of the above challenges. The non-collinear reflections of a ring cavity obviated the need for several bulky isolation optics reducing the size and weight of the sensor. The considerable reduction of parallel surfaces was also observed to reduce optical fringing. Additionally, the choice not to use the NICE-OHMS technique meant that the transmission detector no longer needed a frequency response in the hundreds of MHz, but rather only then tens of kHz. This in turn meant we could increase its size from 100 microns to 1 mm, and reduce fringing still further by alleviating focusing requirements. However, in FY05 further challenges were identified specifically related to the use of the ring cavity, including more difficult alignment procedures and the requirement for specialized piezo mirror mounts to be designed and constructed. These will be dealt with in detail in the following sections.

3.0 The Ring Cavity

3.1 The ring configuration and its advantages

Because of the non-collinear nature of a ring cavity, its use rather than that of a linear standing wave cavity provides a large degree of natural isolation from feedback. The FM recovery sensor based on a ring cavity is shown in Figure 3.1. The incident and reflected fields from the input mirror are no longer coincident due to the circular optical path within the ring resonator. Consequently, the reflected field from the optical cavity no longer reflects directly along the incident path and possibly back into the laser causing the effects of optical feedback and possible damage.

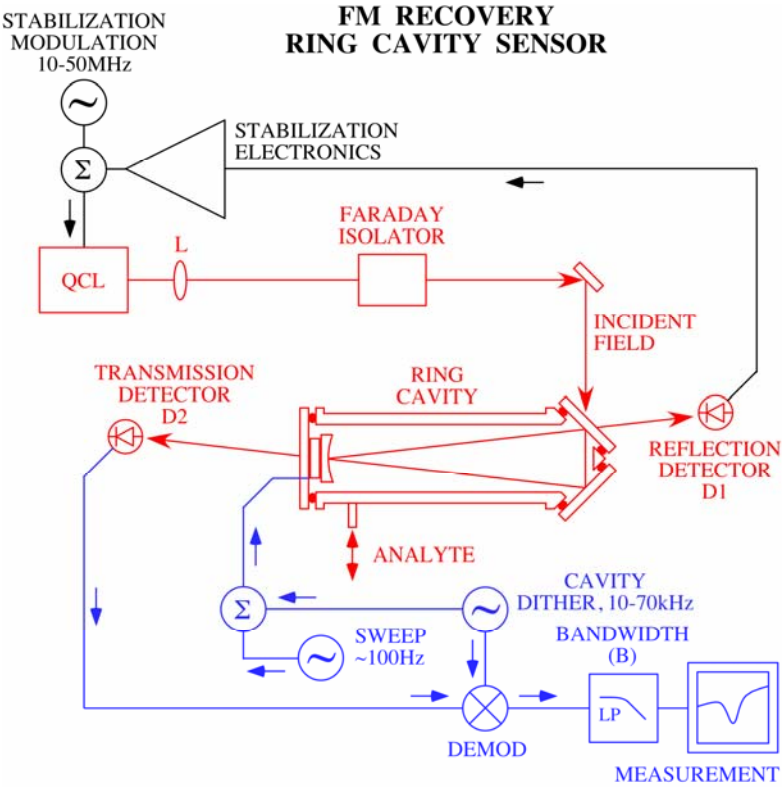

Figure 3.1. Ring Cavity version of the FM Recovery Sensor. The architecture of the ring cavity allows much simplification and reduction of the footprint. Note that the AOM, λ/4 and WGP of Figure 2.2 are missing.

At first glance it seems that this removes the need for isolating components altogether, although this is not true. Back reflections still occur from stray reflections and scattered light from various surfaces. Moreover, direct back-reflections can still occur after the ring cavity and propagate back through it since the cavity is locked and the mode is coupled. However, during FY05 our work showed that this configuration successfully allowed us to dispense with the AOM, the bulky λ/4 rhomb, and the lossy and fragile wire grid polarizer. To illustrate the reduction in footprint and other advantages this yielded, we discuss these components in more detail separately. The AOM itself weighed several pounds, required

water-cooling from a chiller or water faucet, and was driven by 70 Watts of RF power supplied by a large amplifier weighing in at 44 lbs! The λ/4 rhomb weighs at least 1 lb, and is known to cause optical fringing from our previous research. The wire grid polarizer was in fact inadequate as an isolation component and further polarizers were often required, adding again to fringing issues. The combination of λ/4 rhomb and wire grid polarizer deserve further discussion, also serving to highlight yet another problem solved by the ring cavity. Together, these components form an "optical circulator", which in the linear cavity configuration allowed the maximum possible coupling of the input field to a linear cavity, and also of the cavity reflection to the reflection detector. This is achieved by rotating the polarization from linear to circular after reflection from the wire grid polarizer, and then back to linear of the opposite orientation upon reflection from the cavity, so that this reflected field passes through the wire grid polarizer on to the detector. One of the major revelations in FY05 was that this circulation process is far from perfect in our linear cavity arrangements. Specifically, it was found that with the high finesse cavities used, the required angles of orientation of these optics did not correspond to the theoretical optimum values, and adjusting these optics to these angles caused considerable optical feedback. The most likely reason for this is that with the high cavity finesse values used in these sensors, optical striations in the mirror coatings themselves provide a natural polarization preference for the optical cavity. Consequently, it simply doesn't function well with circularly polarized light, necessary for an optical circulator to function. Because of the natural isolating properties of the ring cavity and the fact that we can and must use linear polarization in conjunction with it, its replacement of the linear configuration removes with one stroke both this polarization problem and the need for these inefficient optics. Our research showed however that we still require the Faraday rotator. This unit, built in house is still relatively large and heavy. Its size is due to the requirement for a large and uniform magnetic field (developed by permanent magnets) to interact with a small crystal optic at the center of the device. It also has lower transmission than desired. However, we believe that these properties can be improved with further research and engineering.

3.2 Alignment sensitivity and mirror mounts

Aligning a ring cavity differs from that in a linear cavity in that the beams are not collinear. This not only makes this process more difficult, but also means that if the cavity length is changed, the angles change. Consequently, the mirror mounts we used in the ring had to have a larger range of angular adjustment than those for the linear cavity, which could be mounted firmly at normal incidence. However, the sensitivity to alignment is just as sensitive, and herein lies the first problem we encountered. A picture of the first mount we used is shown in Figure 3.2. The simple construction of this mount is similar to that used in the previous linear cavity system, employing external O–rings and seats, against which the mirrors are held in place by a circular retainer and screws. This arrangement allowed us to test the basic performance of the ring cavity configuration and its feedback impact on the QCL at minimal cost. It was also hoped that it would form the basis for the fieldable design, with only a few modifications to allow one of the mirrors to be swept with a piezo element. During this preliminary testing however, this mounting arrangement proved to be very sensitive to misalignment induced by varying analyte pressure in the cavity chamber, discussed in detail below. Inherent in the ring cavity configuration, are the off-axis reflections from each of the three mirrors. The angular precision required to obtain a stable configuration was unfortunately beyond that obtainable with the simple O-ring seated mount shown in Figure 3.2. To illustrate, when the ring was aligned at atmospheric pressure and then pumped down to 10 Torr, the cavity mode was completely lost. This is in contrast to the linear cavity designs using this type of mount, which stayed very well aligned during such pressure transitions. The

reason for this was the absolutely perpendicular mounting position of the mirrors and consequent even pressure on the whole surface of each of the O-rings. The dihedral mount for the mirrors had to be completely redesigned, as shown in Figure 3.3.

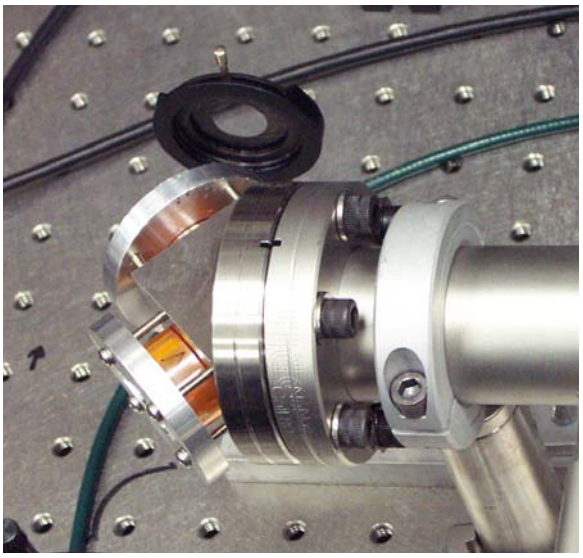

Figure 3.2. This is a picture of the old dihedral mount for the ring cavity. The construction was similar to those used for the linear cavity, using external O-ring mounts, but on a dihedral approximating the reflection angles necessary for the ring cavity. Adjustments to this angle are made via the four screws on each mount. Unfortunately, this is unstable under varying pressure.

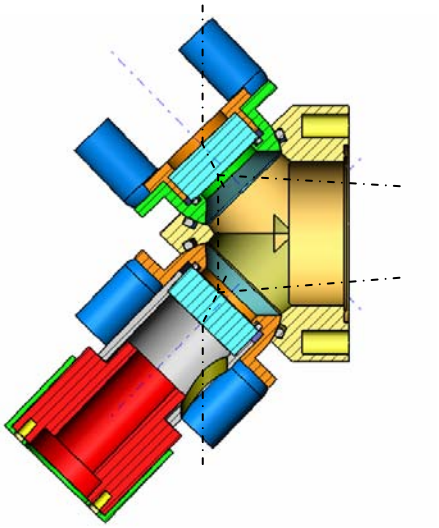

Figure 3.3. Schematic of the new dihedral mirror mount with full mirror angle adjustment yet positive stability. It consists of mirror supports with machined spherical surfaces (orange and green), a center piece with matching surfaces with O-ring grooves (yellow), and precision adjustment screws (blue).

It consists of a modified centerpiece with spherical surfaces machined into the faces (yellow). Mirror supports (orange and green), with matching spherical surfaces were also designed to fit precisely into the dihedral mount. O-rings in grooves machined into the surfaces of the dihedral mount provide a vacuum seal, while allowing unencumbered rotary movement of the mirror mounts. In this way, precise mirror adjustment is thus obtainable under a wide range of pressure conditions. Once the desired alignment is obtained, clamping bolts (blue) are tightened to hold the mirror mounts firmly in place. This is an important capability for the fieldable system, as a certain level of immunity to external forces and movement is essential. One of the mirror supports (bottom) incorporates a commercial piezo device (red) that allows the mirror to move against its O-ring thus providing cavity length adjustment, and an adapter with an exit hole for the transmitted beam, shown in black dashed lines. A picture of the physical realization of this mirror mount is shown in Figure 3.4. The necessity for the fabrication of this mount resulted in the commitment of considerable resources, and resulted in a delay of milestones. In particular, the machining of the matching spherical surfaces required particular time and attention. Preliminary experiments with this new mount show much promise. Alignment shift during depressurization is

minimal. Further work is still required, in particular, some parts may be need to be re-machined in brass to prevent binding due to its natural lubricating properties. When the design is finalized the adjustment screws will be replaced with fine pitch screws to facilitate fine optical adjustment.

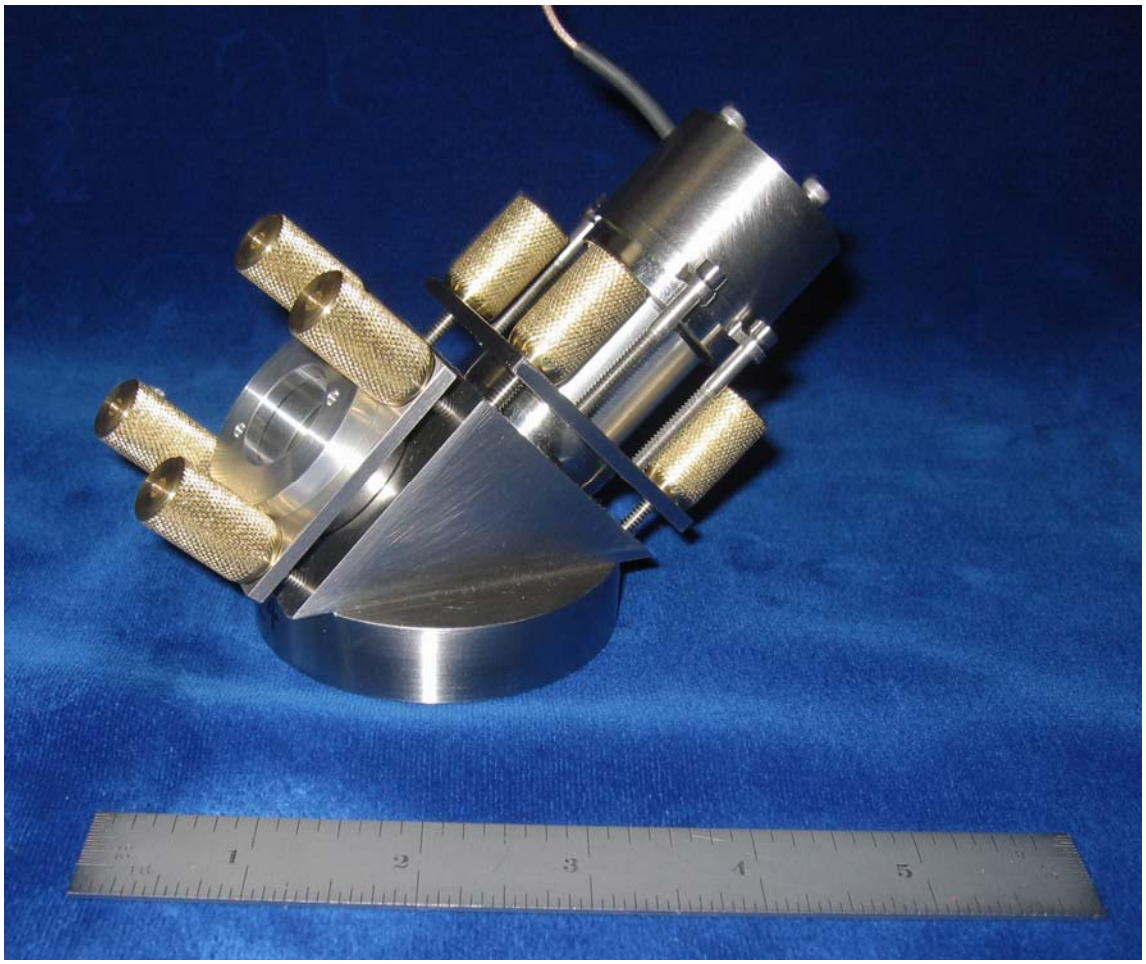

Figure 3.4. Picture of the physical realization of the mount schematic shown in Figure 3.3.

4.0 Cavity Dither

To facilitate the transition from detection of Lamb dip less than a megahertz wide to that of Doppler features 65 MHz wide, an according increase in cavity dither depth was required. Due to the restricted motion afforded by our original design piezo-operated dither mirror mount, a more sophisticated design was required. The result is a mount capable of much greater movement, and the successful recovery of Doppler features.

4.1 The original piezo mirror mount: Lamb dips

Figure 4.1 shows a schematic representation of the original dither mirror mount. Our optical cavity and gas chamber is fabricated from vacuum fittings. A very simple way to make a mirror mount for such a cavity is to machine an O-ring groove into the end plate (magenta), and apply moderate pressure against the mirror (blue) via an annular clamp (red). The internal vacuum of normal operation aids in holding the mirror in place. The ability to rapidly dithering the mirror is afforded simply by adding an annular piezo (yellow) and re-fabricating the clamp from an electrical insulator, macor. This design works superbly for the detection of Lamb dips as shown in Figure 4.2.

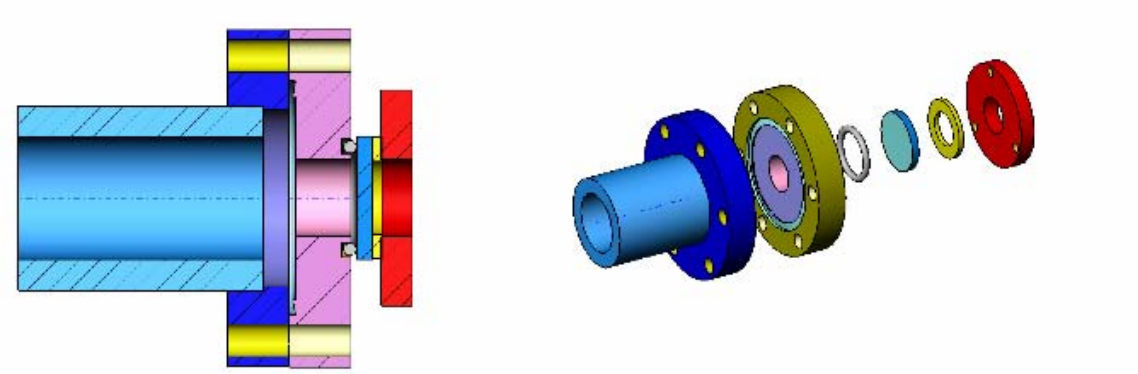

Figure 4.1. Cut-away and exploded views of the original piezo-driven dither mirror mount. The annular piezo disk (yellow) is clamped against the mirror (blue) seated against an O-ring (gray), in turn seated in a groove in the vacuum flange. The O-ring provided enough elasticity and frequency response to allow adequate modulation at up to 60 kHz to achieve a 1 MHz modulation depth, optimal for Lamb dip recovery but inadequate for Doppler signal recovery.

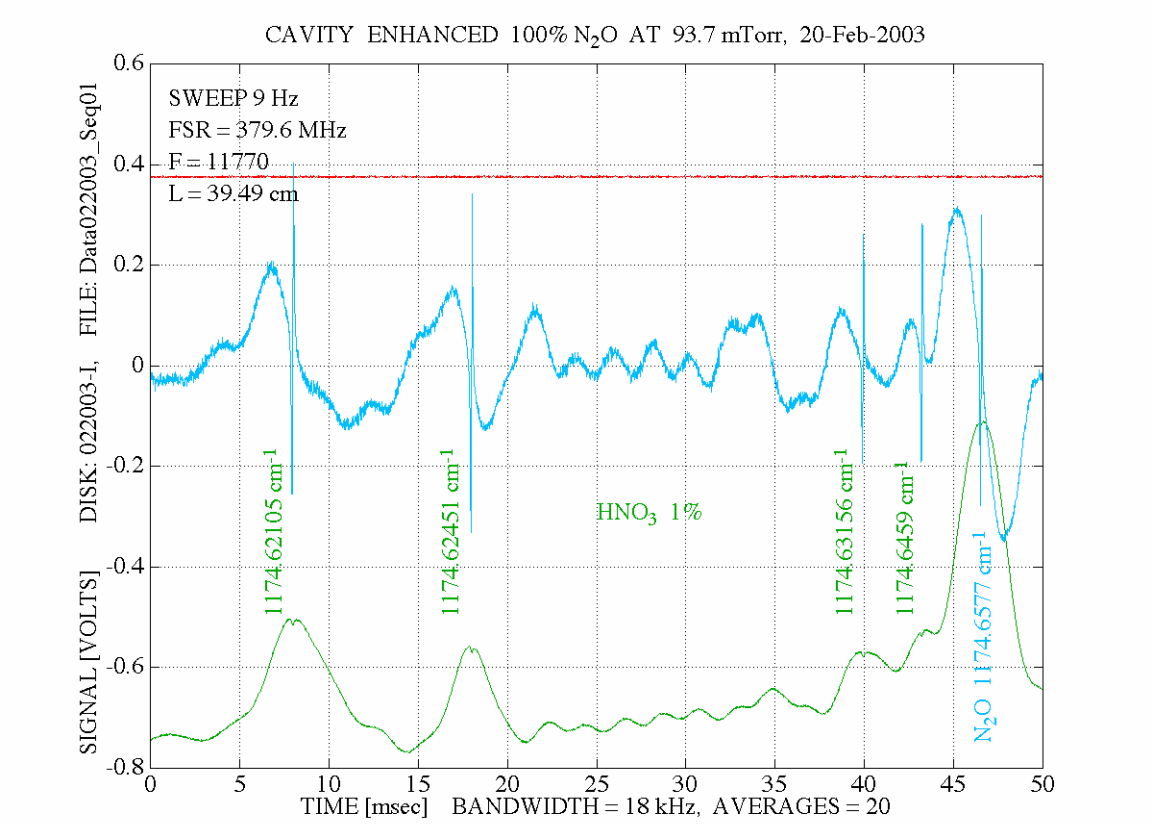

Figure 4.2. This figure shows results of the cavity-dither FM recovery system optimized for Lamb dips in blue. For comparison, the DC cavity-locked detection signal is shown in green with the corresponding zero transmission trace shown in red. While the Lamb dips are visible in the DC transmission trace, they are clearly very much amplified in the FM recovery trace. Features labeled in green are due to 1% nitric acid contamination (HNO_3) of what we thought was a pure 100% nitrous oxide (N_2O) sample. One N2O line is shown labeled in blue to the right.

4.2 The re-designed piezo mirror mount: Doppler features

The original arrangement shown in Figure 4.1 is optimized for Lamb dips. It cannot however cause deep enough excursions to successfully recover the Doppler signals. As can be seen in Figure 4.2, the Doppler features themselves are clearly of non-optimal signal-to-noise. The new design of the piezo cavity-dither mirror mount is shown in Figure 4.3. In this arrangement, the mirror and piezo are entirely internal to the housing, and a window (not shown) is used to make the vacuum seal. The result is that the mirror has superior movement.

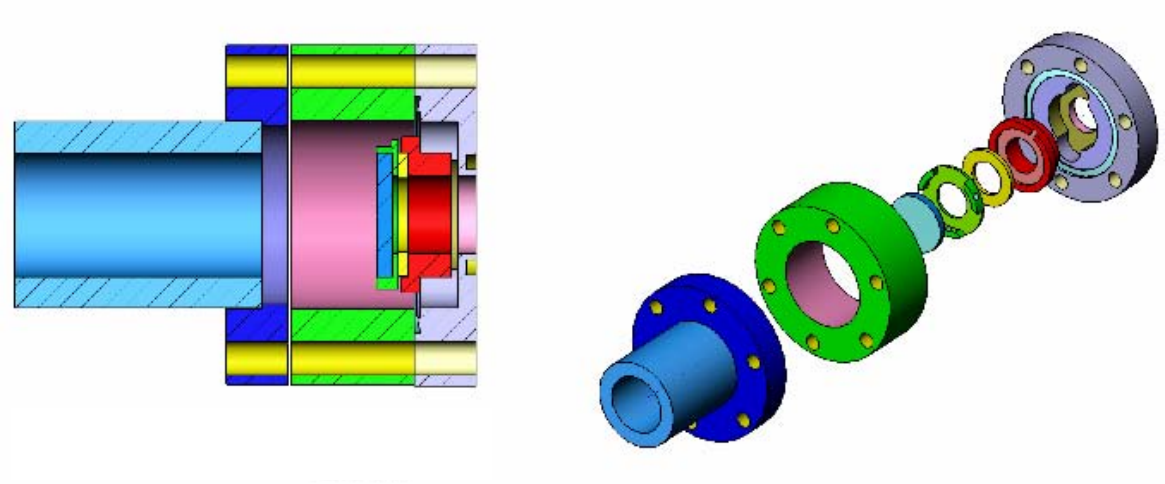

Figure 4.3. Cut-away and exploded views of the new piezo and mirror mount design, which is internal to the low-pressure gas cell. The O-ring remains external and will now be in contact with a BaF window (not shown) rather than the mirror in order to form the vacuum seal. The mirror (blue) is mounted in a thin aluminum cup (green), glued to the annular piezo disk (yellow), which is in turn glued to a macor ceramic insert (red) for electrical insulation, which is screwed into the vacuum flange. An electrical feed-through (also not shown) is now needed to pass the signal to the piezo disk inside the chamber.

The success of this arrangement is demonstrated in Figure 4.4 below, a scan of a Doppler-broadened N_2O transition, approximate FWHM 65 MHz. The DC transmission trace (blue) again shows the Lamb dip as before. However, the cavity-dither FM recovery trace (blue) now shows the width of the Doppler feature, and no evidence of the Lamb dip. The comparison of Figures 4.2 and 4.4 shows the potential of the FM modulation technique to differentiate between signals of different spectral widths, the Lamb dips being dominant in Figure 4.2 and the Doppler features in Figure 4.4. One disadvantage of the deep-dither technique is that we cannot modulate the piezo at a rate as rapid as for the original design, the dither frequency being reduced from around 40 kHz down to 2.42 kHz. The result is a reduction in maximum scan rate due to the necessity of smaller filter bandwidth to remove interference at the modulation frequency. Nevertheless, the data in Figure 4.4 still represents parts-per-trillion relative concentration detection of N_2O in a fraction of a second.

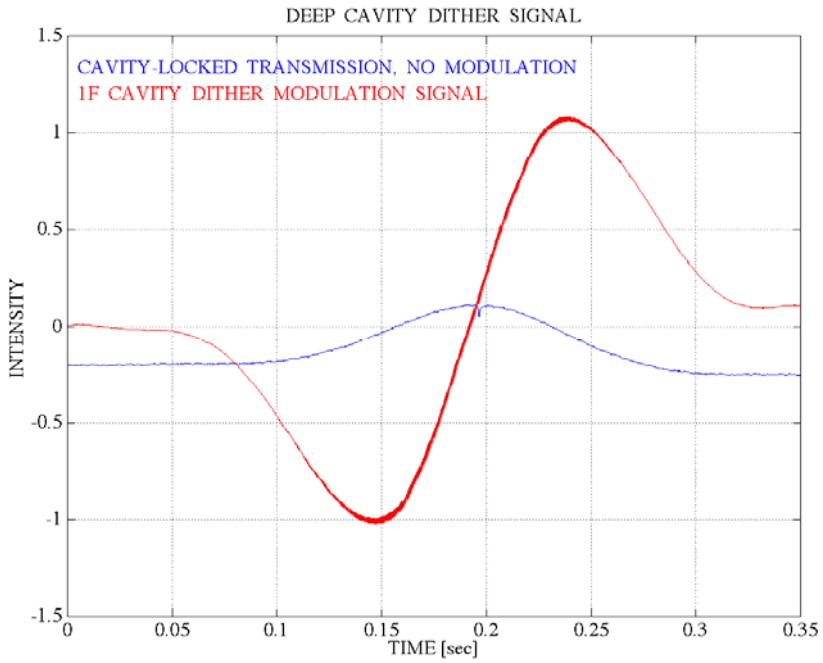

Figure 4.4. Shows deep-dither FM recovery cavity-locked signals of a Doppler-broadened N_2O transition, being about 65 MHz FWHM. The blue trace shows the DC cavity transmission with the modulation off; the Lamb dip is clearly visible. The red trace shows the FM signal with a modulation depth of around 10 MHz; the response favors the Doppler feature rather than the Lamb dip, which is no longer visible at all. Dither frequency was 2.42 kHz.

5.0 The modified laser dewar

In FY04 a complete redesign of the laser dewars took place. The reason for this was that the in design of the existing dewar, purchased from Laser Components for around $6k, the inner reservoir was secured to the top of the outer skin of the dewar via the filler neck. Consequently, as the dewar heated and cooled, the base of the inner chamber where the QCL is generally mounted, moved up and down relative to the outer skin and thus the exit window and external optics by up to 0.8 millimeters. There was also considerable pendulum motion of this plate. With the advent of vastly improved coupling lenses mounted on extender tubes reaching into the dewar and allowing the lens to be placed immediately next to the QCL output facet (thus greatly improving the optical coupling), this movement in the laser mounting plate meant significant misalignment of optical systems both with thermal cycling of the laser dewar, but also during any one day of operating as the liquid nitrogen boiled off. During the initial investigation of the available detection techniques with our LWIRCES system, some alignment drift in the laser dewars was tolerable. However, in moving forward to a fieldable design, this movement was detrimental. The new design rectifies this problem by securing the laser mounting plate and thus the base of the inner vessel to the base of the output skin in a thermally insulating manner, and extending the top of the dewar allowing stainless steel bellows to be installed between the top of the inner vessel and the filler hole. The details of this process are covered in detail in section 3.1 of the FY04 annual report, but stability tests were not performed until FY05.

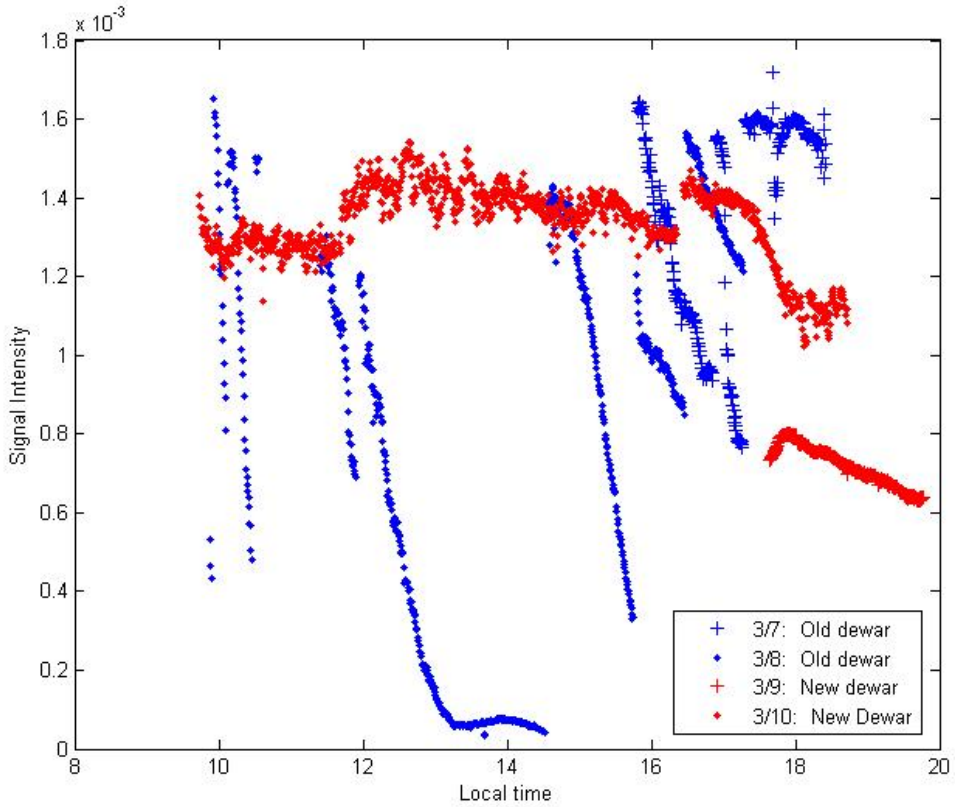

Figure 5.1. Scatter graph showing QCL returns from a corner cube located 1500 meters away. Clearly at this distance, misalignments have a large impact. The data shown in blue was taken using an unmodified laser dewar, showing several dropouts where realignment had to be performed. The data in red was taken using the modified dewar, and shows much more stable behavior.

5.1 Results of stability tests

The resulting stability is far better than the unmodified dewar. Figure 5.1 shows a scatter graph of intensity vs. time local time in hours of QCL returns from a corner-cube over a total path length of 1500 meters. The blue data are two daylong tests of an un-modified version of the dewar, while the red data are two tests of the modified dewar. The discontinuities are where the experiment had to be stopped, and the alignment readjusted. It is clear that the new dewar has superior stability, and although there was one manual readjustment, the return intensity never falls to zero as it does in the unmodified case. In addition, the lower red data set to the right is believed to actually be an atmospheric event rather than a misalignment.

6.0 Optimization of the QCL current supply

One of the major achievements in FY02 was the successful design and implementation of a low noise QCL current supply. One of the principal ways to vary the frequency and intensity of any semiconductor laser is to vary the injection current. Consequently, noise or long term instability on the drive current results in similar undesirable characteristics appearing on the QCL output frequency and intensity. At the end of FY02, our current supply exhibited an already low value of current noise of around $10nA/Hz^{1/2}$ at 10 Hz. QCLs operating with this power supply exhibited free running laser line-widths of around 100 kHz (Myers et al. 2002), compared to over a megahertz when operating from previous versions. (Typical "low noise" power supplies on the market have current noise of a few microamperes.) This 100 kHz line-width is of the order of the transit time broadening seen inside the optical cavities we use for the LWIR-CES, the beam being about one millimeter in cross section, which is about the minimum useful line width we can expect to find useful in LWIR-CES, and then only when used in conjunction with sub-Doppler features such as Lamb dips. Nevertheless, there was still considerable work to be done to make the current supply stand up to commercial units in all aspects, including the long-term stability of the unit. The combined demands placed on the design of the QCL current controller for this and other projects, resulted in a difficult design task. Not only does the QCL have to be low noise, it must be stable in the long term, resulting in minimum drift of the current over a period of minutes or hours. Additionally, when required, the current supply must be able to sweep over a considerable proportion of its operating current at rates up to tens or even hundreds of kHz to fully utilize the deep modulation characteristics of QCLs. Work has continued over the last several years to satisfy this demanding set of constraints, and in particular, major modifications were made to each part or module of the design in FY04, a full account of these modifications being given in section 4.0 of the FY04 annual report (Taubman et al. 2004a). In FY05 new units incorporating these modifications were produced, and we report here on the performance of these units.

6.1 Performance and comparison to commercial units

Figure 6.1 shows the four principal test configurations used to evaluate the QCL5 controller. All these configurations involve using a low temperature coefficient 10Ω resistor R to convert the output current to a voltage signal that can then be examined for noise levels, transfer function, long term stability and speed of deep modulation. Each of these properties is discussed separately in the sections to follow.

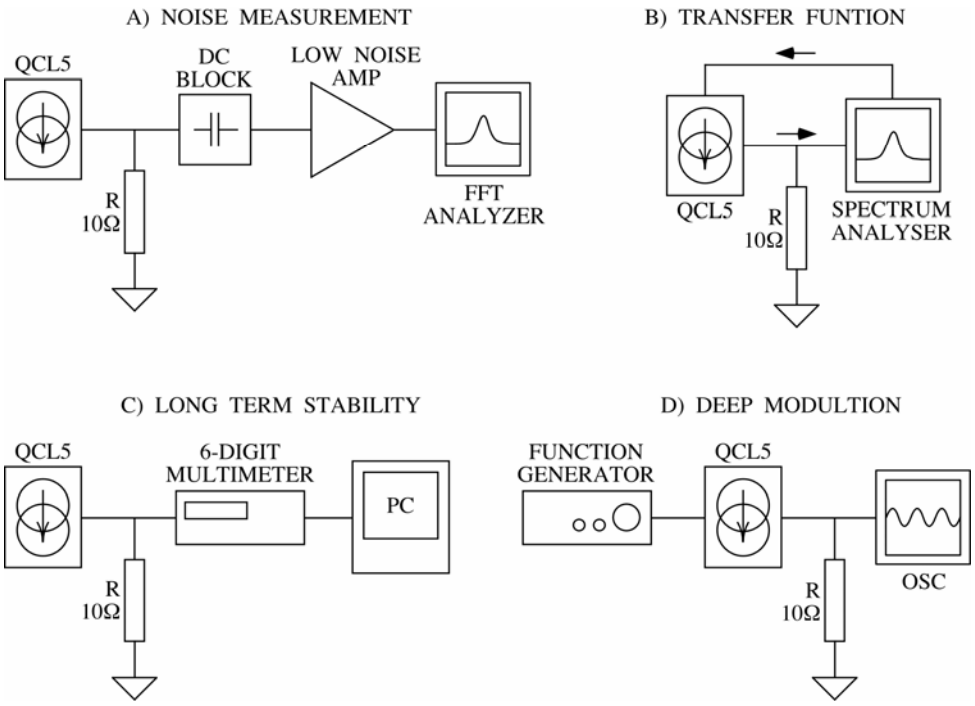

Figure 6.1. Test configurations for the QCL5 current controller. All arrangements use a precision low temperature coefficient power resistor to produce a reliable voltage signal from the output current. In A), only the fluctuations of this voltage pass through a DC block and into a Stanford Research SR560 low noise-voltage amplifier, and then to a SR785 FFT analyzer. In B), the tracking generator function of an Agilent E7402A spectrum analyzer is used to facilitate measurement of the slow and fast amplitude transfer functions. C) shows the long-term stability configuration, which uses an Agilent 34401A 6-digit multimeter operated via a PC running Labview. D) shows a function generator and an oscilloscope used to test the deep-modulation response of the unit.

6.1.1 Noise Performances

The noise performance of the QCL5 was measured by configuration A) shown in Figure 6.1. The current fluctuations were converted to voltage fluctuations by the precision 10W resistor, and passed via the DC block into a low noise voltage amplifier and then to a precision FFT analyzer. The results of this measurement (red) along with those from similar noise measurements conducted on two commercial units (magenta and green) are shown in Figure 6.2.

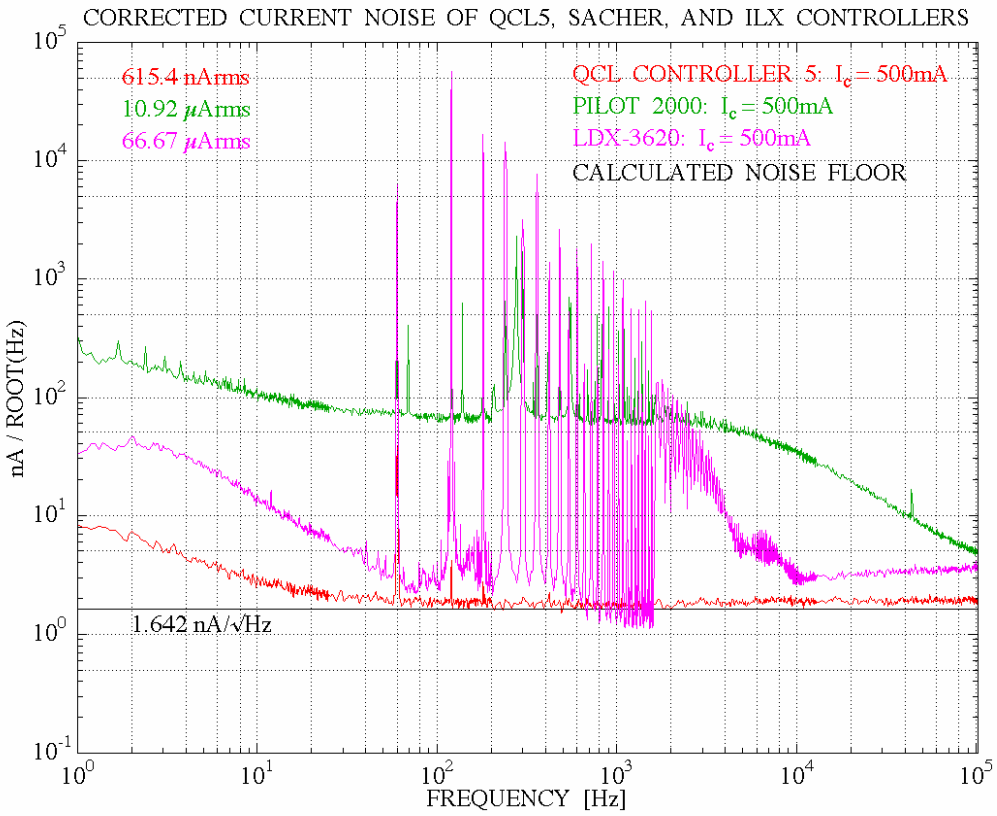

Figure 6.2. Noise spectra of the QCL5 (red), and two commercial units, the Sacher Lasertecknique Pilot 2000 (green) and the ILXlightwave LDX-3620. The minimum theoretical noise level of the QCL5 based on the Johnson and shot noise of internal resistors and transistors is also shown in black. The noise levels are "corrected" for the residual noise of the measurement apparatus by subtracting this noise in quadrature.

The theoretical lower limit to the QCL5 noise level is also in black. The most striking feature is that the noise of the QCL5 (red) drops very close to the theoretical noise level of 1.64 nA/√Hz at a low spectral frequency of around 40 Hz, and remains there out to 100 kHz, one of the most critical regions where laser performance can be deleteriously affected. The Pilot 2000 (green) exhibits noise approximately 30 times this value and an oscillation at around 280 Hz. The LDX-3620 (magenta) exhibits so many interference peaks from 60 Hz line noise and its harmonics, that it disrupts the measurement of the true noise floor of this supply, although it may approach this same value. This many interference peaks however, are detrimental. This translates into an rms noise values of 4.2µArms for the full 5 MHz noise bandwidth of the unit, or 620 nA/√Hz if the response is limited to 100 kHz with an appropriate output filter.

6.1.2 Transfer Function

The transfer function of the current supply is essentially the response of the output of the unit to a given input. This test was performed using configuration B) of Figure 6.1. An output signal from the tracking generator of a spectrum analyzer specifically meant for such measurements, was fed to the input (either fast or slow) of the QCL5. The output is then measured by the analyzer. Transfer function is significant because QCLs can be rapidly modulated. Usually current supplies don't have a frequency response beyond 100 kHz or so, meaning that higher modulation frequencies need to be applied via other methods including bias-T networks. While this is in general not a problem, this unit allows useful response of its slow and fast inputs out to 5 MHz and 70 MHz respectively facilitating such modulation without the use of other networks, avoiding any unforeseen interference effects. This transfer function performance is seen in figure 6.3. No other responses of the commercial units are shown here, because they cannot be sensibly displayed on the same graph, being up to three orders of magnitude slower, for example the Pilot 2000 rolls off at 10 kHz.

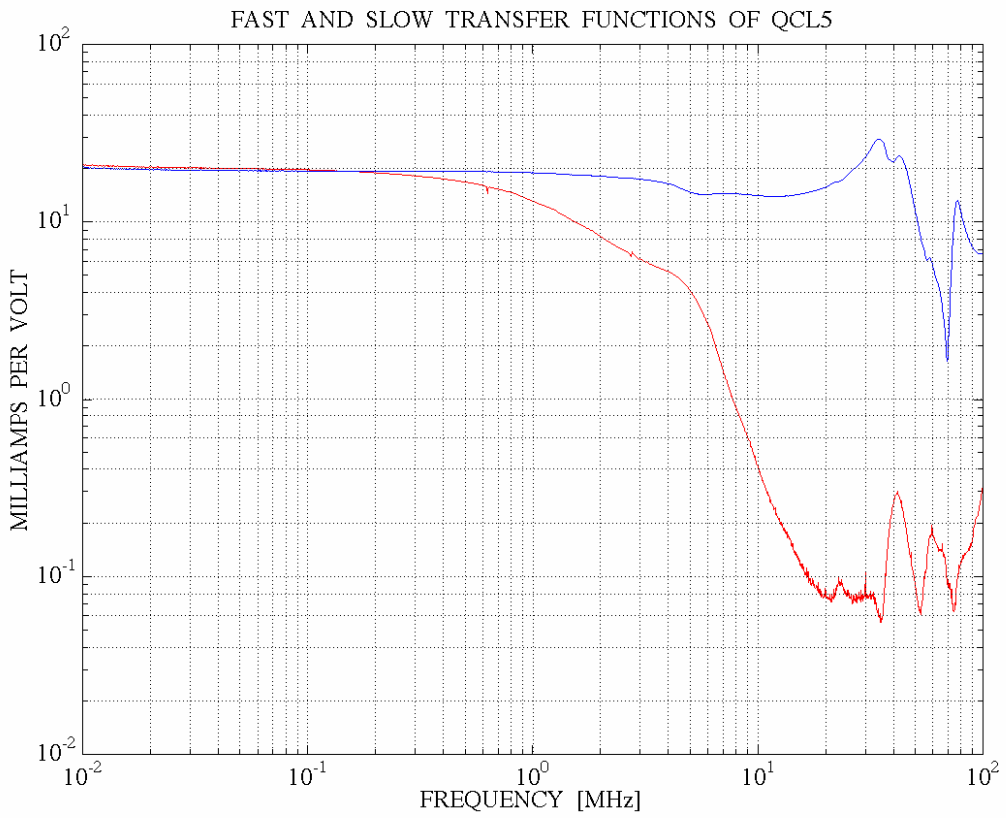

Figure 6.3. This figure shows the transfer functions of the slow (red) and fast (blue) transfer functions of the QCL5. They exhibit 3 dB rolloff points at 1 MHz and 10 MHz respectively, and 14 dB rolloff points at 5 MHz and 70 MHz.

6.1.3 Long term Stability

The ability to continue to produce the same current levels through varying temperatures translates directly into the ability of the QCL to be held on a given frequency, provided other parameters of the laser are controlled in particular its operating temperature. This is important for a fieldable sensor, because it implies the ability of the sensor to reliably target the same spectral features continually despite varying environmental conditions. The long-term stability measurements were performed using the configuration shown in C) in Figure 6.1. The voltage expressed across the precision resistor was monitored by a 6-digit multimeter, linked to a computer. Figure 6.4 shows the results of the long-term stability measurements of the QCL5 compared to those of the two commercial units being tested. The QCL5 clearly exhibits superior stability performance.

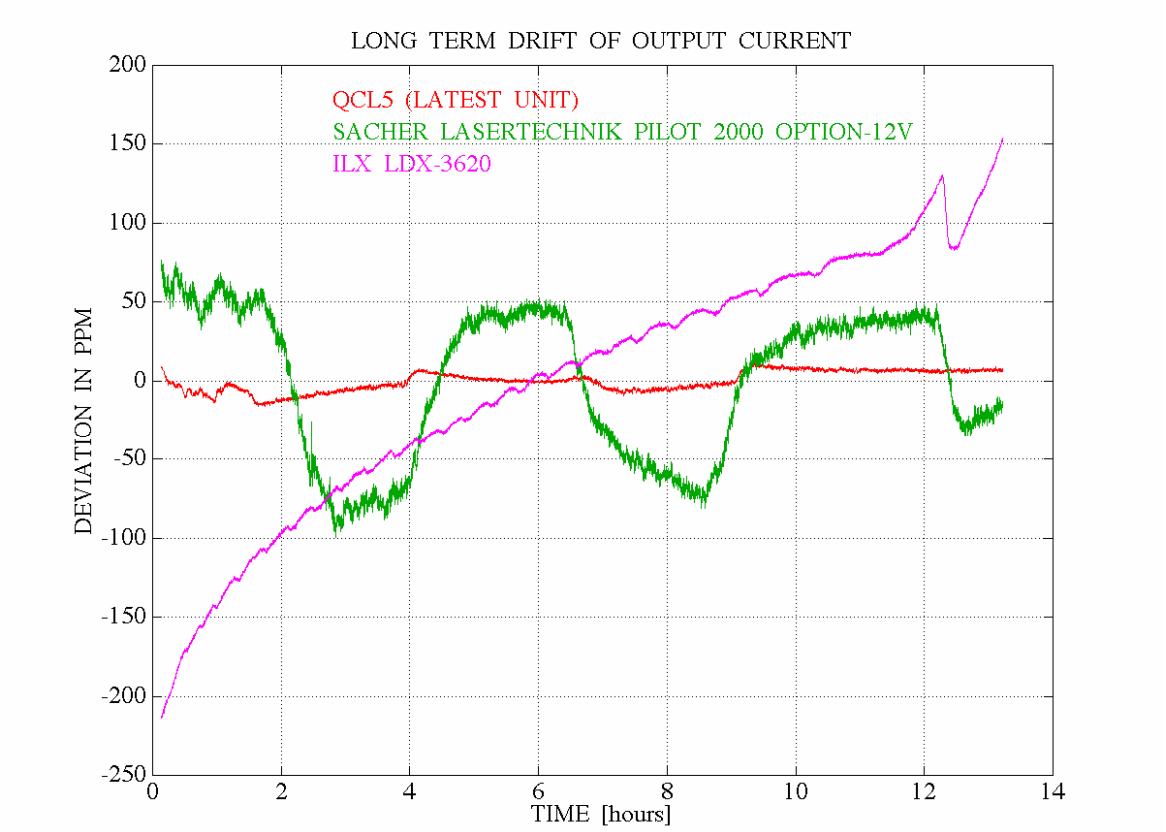

Figure 6.4. Plot of long-term stability of the QCL5 (red), the Sacher Lasertecknique Pilot 2000 (green) and the ILXlightwave LDX-3620 (magenta), over just over 13 hours of continuous operation over night in our laboratory. The QCL5 shows a long-term variation of 20 parts-per-million (ppm) peak-to-peak, while the peak-to-peak variations of the Pilot 2000 and LDX-3620 were 150 ppm and 350 ppm respectively. Moreover, the LDX-3620 shows some kind of long-term drift behavior unrelated to external temperature conditions. The temperature variations in the laboratory corresponding to these measurements was around one degree Celsius.

6.1.4 Deep Modulation

QCLs can be modulated rapidly and deeply. In order to utilize this ability, the QCL5 current controller can respond full scale to square wave input out to 100 kHz. This measurement is performed by driving the unit with a signal generator and observing the response with an oscilloscope as shown in D) of Figure 6.1. The response to this test is shown in Figure 6.5. The corners are slightly rounded because the internal regulator was not specifically designed for pulsed operation, but this is still very much faster than most commercial units. This response can be improved if so desired at the expense of some noise performance, to make the unit more suitable for arbitrary-shape pulsed operation.

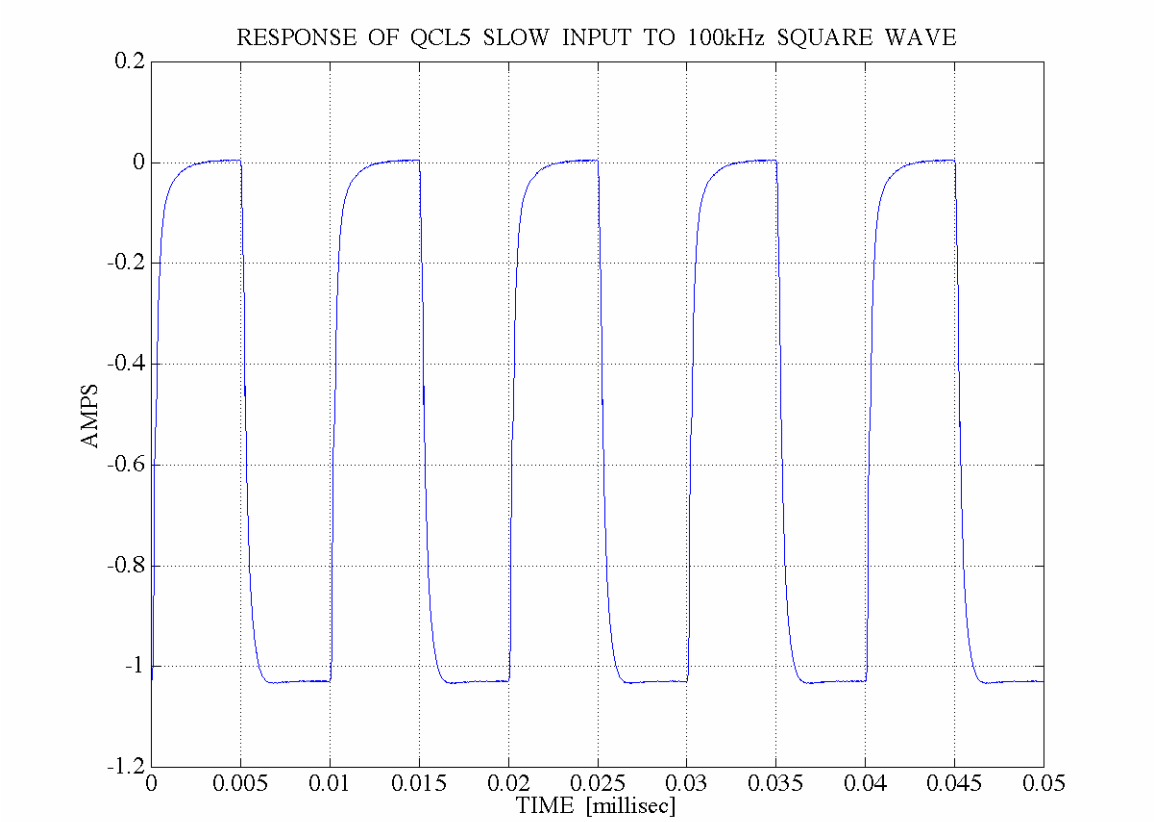

Figure 6.5. Shows the full response of the QCL5 (1 ampere peak-to-peak) to a 100 kHz square wave applied to the slow input.

These four different measurements show the QCL5's superior performance compared to at least two commercially available units, sold as low noise precision supplies. The QCL5 exhibits a noise level almost reaching the theoretically attainable values, and is agile and stable.

7.0 Plans for FY06

7.1 Discussion and synopsis of state-of-the-art chemical sensing

There are many important sensing applications in world today. Even amongst those relating to national and global security there are applications of different sensitivity and selectivity, not to mention levels of false positives or negatives. To satisfy this need there are many different sensor configurations, of which the various cavity-enhanced sensor architectures shown in this report represent a small subset. Others include direct detection without the benefit of an optical cavity, either at DC or some modulation frequency, the use of delay lines such as White or Herriot cells, which give a sensor similar advantages to using an optical cavity, but with different tradeoffs. Another important innovation is the use of preconcentrators and catalytic converters to amplify the utility of chemical sensors. The use of smart materials in conjunction with this technology makes it possible to make sensors tuned strongly tuned to specific analytes, which could be an excellent way of avoiding the effects of interference from unwanted signatures. Since some of the possible configurations are extremely compelling, for FY06 besides continuing developing the ring cavity-locked sensor with deep dither modulation, we will be conducting preliminary tests of a complementary sensor, that of simple direct absorption detection using a highly promising modulation technique unable to be used in conjunction with optical cavities, and possibly combined with a preconcentrator or catalytic converter. This technology could prove very suitable for smaller scale systems requiring high reliability and moderate sensitivity.

7.2 Two architectures for a range of applications

7.2.1 The ring cavity-dithered FM recovery sensor

With the work completed in FY04 and FY05 we are now close to fielding this sensor. There are minor refinements and modifications to be made to the new mirror mounts. There will be some additional electronics to be constructed to operate the deep cavity dither system more effectively, and refinement of detector preamplifier circuitry. We will then focus on optimizing the layout and setting up the data acquisition system for our first field tests. The first field test will be with a manually operated locking system, as development of the automatic locking system was delayed from FY05 to late FY06 or FY07.

7.2.2 Direct detection using two-tone modulation

The modulation technique we propose to try during FY06 is that of direct detection using two-tone modulation depicted in Figure 7.1, and an effectively equivalent technique we refer to as three-tone modulation in Figure 7.2, which may be easier to perform in the laboratory depending on the equipment available.

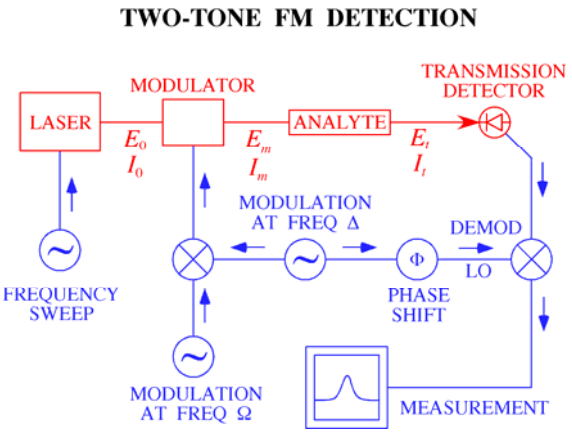

Figure 7.1. The two-tone technique involves applying two different tones to the laser but detecting at the difference frequency.

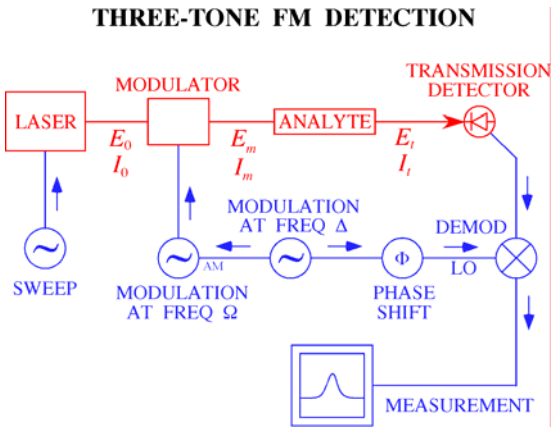

Figure 7.2. An equivalent technique to two-tone, except the AM modulation input of most signal generators is used to effectively generate three tones, the detection process again occurring at the difference frequency between adjacent tones.

The advantages of the two-tone technique as opposed to other FM techniques we have used over the previous years are primarily involved with modulation levels and optimal noise regions of detectors. The average modulation frequency can be selected to be outside the line width of the molecular absorption features being targeted, say 100 MHz or so, which has the important advantage that the optimal modulation depth required is actually quite a small, typically a radian of phase change. This is relatively easy to generate, and causes minimum disruption to QCL operation. However, as we have shown in the past (FY03 report) that MCT detectors have a poor response at high frequencies. This is no longer a problem with two-tone detection, as the detection process is carried out at the difference between the two tones, which could be as low as tens of kHz, well within the optimal response region of MCT detectors, but to be chosen above any region technical noise inside the detector element or preamplifier electronics. A further advantage of this technique is that largely because it is a second order technique, two-tone detection has a greater immunity against residual amplitude modulation (RAM), which occurs whenever a QCL is frequency modulated. RAM causes spurious signals that mask those representing genuine absorption events. QCLs are particularly prone to RAM effects, because of their low alpha parameter[1] (Faist et al. 1994; Yariv 1989; Henry 1982). Over FY06 we intend to ascertain whether the two-tone or equivalent three-tone technique is as powerful as it appears, and whether it is prudent to pursue a sensor based on this technique, possibly also including a preconcentrator or catalytic converter unit.

[1] The alpha parameter is basically the relationship between amplitude and phase behavior of the laser. The smaller this value, the less amplitude fluctuations accompany phase changes. Consequently, demanding a particular phase modulation produces more accompanying amplitude modulation.

8.0 Summary and Outlook

Over FY05 we have made progress that greatly reduces the footprint of the cavity-locked sensor to be fielded in FY06 or early FY07 given current funding levels. The specific changes include the implementation of a ring cavity rather than a linear cavity, resulting in the removal of several large optics, which combined with the non-parallel mirrors of the ring, greatly reduce the effects of fringing. The optics to be removed from the sensor design include an acousto-optics modulator, representing a decrease in fieldable weight of greater than 45 lbs, a quarter-wave rhomb, responsible for significant optical fringing, and a wire grid polarizer, which is fragile and lossy. Unforeseen complications due to changing alignment of the ring cavity with pressure were addressed by designing and fabricating a superior mirror mount, which in itself represents significant intellectual property. The resulting ring cavity is far more stable, although minor changes are required to optimize fine alignment capability. The cavity dither technique was successfully optimized for the detection of Doppler features rather than Lamb dips, which required designing and constructing a new piezo-mediated mirror dither mount. This new mount has been shown to be successful, allowing the recording of low signal-to-noise FM recovery Doppler features. It should be mentioned that milestones originally included in our FY05 statement of work were delayed due to a reduction in funding. The unforeseen necessity to redesign the dihedral ring mirror mount accentuated this delay. It is hoped that sufficient funding is available to allow us to field a version of this sensor late in FY06 or in FY07.

9.0 References

Barger RL, M.S. Sorem, and J.L. Hall 1973. "Frequency stabilization of a cw dye laser." *Appl. Phys. Lett.* **22,** 573-575.

Drever RWP, JL Hall, FV Kowalski, J Hough, GM Ford, AJ Munley and H Ward 1983. "Laser phase and frequency stabilization using an optical resonator." *Appl. Phys. B.* **31,** 97-105.

Faist J, F Capasso, DL Sivco, C Sirtori, AL Hutchinson and AY Cho 1994. "Quantum cascade laser." *Science* **264,** 553-556.

Gianfrani L, RW Fox, and L Hollberg 1999. "Cavity-Enhanced Absorption Spectroscopy of Molecular Oxygen." *J. Opt. Soc. Am. B*, **16**(12) 2247-2254.

Henry, CH 1982. "Theory of the Linewidth of Semiconductor-Lasers." *IEEE. J. Quant. Elect.* QE-18, 259-264.

Hjelme DR, S Neegård, and E Vartdal 1995. "Optical interference fringe reduction in frequency-modulation spectroscopy experiments." *Opt. Lett.*, **20**(16), 1731-1733.

Ishibashi C and H Sasada 1999. "Highly Sensitive Cavity-Enhanced Sub-Doppler Spectroscopy of a Molecular Overtone Band with a 1.66 mm Tunable Diode Laser." *Jpn. J. Appl. Phys.* **38,** 920-922.

Loewenstein M, H Jost, J Grose, J Eilers, D Lynch, S Jensen, and J Marmie 2002. "Argus: a new instrument for the measurement of the stratospheric dynamical tracers, N20 and CH4." *Spectrochim. Acta A., Mol. Biomol. Spectrosc.*, **58**(11), 2329-2345.

Myers TL, RM Williams, MS Taubman, C Gmachl, F Capasso, DL Sivco, JN Baillargeon, and AY Cho 2002. "Free-running frequency stability of mid-infrared quantum cascade lasers." *Opt. Lett.*, **27**(3), 170-172.

Salomon CH, D Hils, and JL Hall 1988. "Laser stabilization at the millihertz level." *J. Opt. Soc. Am. B.* **5,** 1576-1587.

Taubman MS, TL Myers, BD Cannon, RM Williams, and JF Schultz. 2002a. "*Ultra-Trace Chemical Sensing with Long-Wave Infrared Cavity-Enhanced Spectroscopic Sensors.*" PNNL-14201, Pacific Northwest National Laboratory, Richland, WA.

Taubman MS, TL Myers, BD Cannon, RM Williams, F Capasso, C Gmachl, DL Sivco, and AY Cho 2002b. "Frequency stabilization of quantum cascade lasers by use of optical cavities." *Opt. Lett.*, **27**(24), 2164-2166.

Taubman MS, BD Cannon, TL Myers, CA Bonebrake, PM Aker, and JF Schultz. 2003. *Long Wave Infrared Cavity Enhanced Sensors.* PNNL-14484, Pacific Northwest National Laboratory, Richland, WA.

Taubman MS, DC Scott, BD Cannon, TL Myers, CA Bonebrake, PM Aker, MD Wojcik, JT Munley, VT Nguyen, and JF Schultz. 2004a. *Long Wave Infrared Cavity Enhanced Sensors.* PNNL-15103, Pacific Northwest National Laboratory, Richland, WA.

Taubman MS, TL Myers, BD Cannon, and RM Williams 2004b. "Stabilization, injection and control of quantum cascade lasers, and their application to chemical sensing in the infrared." *Spectrochim. Acta, A*, **60,** 3457-3468.

Vahala K and A Yariv 1983. "Semiclassical Theory of Noise in Semiconductor-Lasers." *IEEE. J. Quant. Elect. QE*-**19**(6), 1096-1101.

Webster CR 1985. "'Brewster-plate spoiler: a novel method for reducing the amplitude of interference fringes that limit tunable-laser absorption sensitivities." *J. Opt. Soc. Am. B*, **2**(9), 1464-1470.

Williams RM, JF Kelly, JS Hartman, SW Sharpe, MS Taubman, JL Hall, F Capasso, C Gmachl, DL Sivco, JN Baillargeon, and AY Cho 1999. "Kilohertz linewidth from frequency-stabilized mid-infrared quantum cascade lasers." *Opt. Lett*., **24**(24), 1844-1847.

Yariv A 1989. *Quantum Electronics*, 3rd ed. John Wiley & Sons, New York, p. 577-597.

Ye J, L-S Ma, and JL Hall 1998. "Ultrasensitive detections in atomic and molecular physics: demonstration in molecular overtone spectroscopy." *J. Opt. Soc. Am. B*, **15**(1), 6-15.

Distribution

No. of Copies

OFFSITE

LTC Ariel Cuadrado
United States DOE
NNSA/NA-22
1000 Independence Ave. SW
Washington, DC 20585

Dr. Rhys M. Williams
United States DOE
NNSA/NA-22
1000 Independence Ave. SW
Washington, DC 20585

Dr. David Berry
United States DOE
NNSA/NA-22
1000 Independence Ave. SW
Washington, DC 20585

Mr. Ralph Hastings
United States DOE
NNSA/NA-22
1000 Independence Ave. SW
Washington, DC 20585

Mr. Eric Sander
United States DOE
NNSA/NA-22
1000 Independence Ave. SW
Washington, DC 20585

Mr. W. Randy Bell
United States DOE
NNSA/NA-22
1000 Independence Ave. SW
Washington, DC 20585

No. of Copies

Professor Henryk Temkin
Program Manager
DARPA, MTO
3701 N. Fairfax Dr.
Arlington, VA 22203-1714

ONSITE

32 **Pacific Northwest National Laboratory**

Anheier, NC	K5-25
Bruckner-Lea, C	K5-25
Cannon, BD	K5-25
Clemmer, RG	K8-29
Dudder, GB	K8-29
Harper, WW	K5-25
Johnson, BR	K6-24
Munley, JT	K6-24
Myers, TL	K5-25
Nguyen, VT	K5-10
Scott, DC	K5-25
Schultz, JF (10)	K5-25
Sharpe, SW	K8-88
Stewart, TL	K5-25
Strasburg, JD	K5-25
Taubman, MS	K5-25
Information Release Office (7)	K1-06